Original Article

The potential treatment of N-acetylcysteine as an antioxidant in the radiation-induced heart disease

Yan-Ling Li[1,2#], Gang Wang[3#], Bo-Wen Wang[1,2], Yong-Hong Li[4], Yong-Xia Ma[5], Yuan Huang[6], Wen-Ting Yan[6], Ping Xie[1,2,3]

[1]School of Traditional Chinese and Western Medicine, Gansu University of Chinese Medicine, Lanzhou, China; [2]Department of Cardiovascular Medicine, Gansu Provincial Hospital, Lanzhou, China; [3]The First School of Clinical Medicine, Lanzhou University, Lanzhou, China; [4]The Institute of Clinical Research and Translational Medicine, Gansu Provincial Hospital, Lanzhou, China; [5]Department of Cardiovascular Medicine, The Second People's Hospital of Lanzhou City, Lanzhou, China; [6]The First Clinical Medical College, Gansu University of Chinese Medicine, Lanzhou, China

Contributions: (I) Conception and design: P Xie, YL Li; (II) Administrative support: P Xie, YH Li; (III) Provision of study materials or patients: Y Huang, WT Yan; (IV) Collection and assembly of data: YL Li, G Wang, BW Wang; (V) Data analysis and interpretation: YH Li, YX Ma, Y Huang, WT Yan; (VI) Manuscript writing: All authors; (VII) Final approval of manuscript: All authors.

[#]These authors contributed equally to this work.

Correspondence to: Dr. Ping Xie, MD, PhD. School of Traditional Chinese and Western Medicine, Gansu University of Chinese Medicine, Lanzhou 730000, China; Department of Cardiovascular Medicine, Gansu Provincial Hospital, No. 204 Donggang West Road, Lanzhou 730000, China; The First School of Clinical Medicine, Lanzhou University, Lanzhou 730000, China. Email: Pingx189@outlook.com.

Background: Radiation-induced heart disease (RIHD) is a serious complication of thoracic tumor radiotherapy that substantially affects the quality of life of cancer patients. Oxidative stress plays a pivotal role in the occurrence and progression of RIHD, which prompted our investigation of an innovative approach for treating RIHD using antioxidant therapy.

Methods: We used 8-week-old male Sprague-Dawley (SD) rats as experimental animals and H9C2 cells as experimental cells. N-acetylcysteine (NAC) was used as an antioxidant to treat H9C2 cells after X-ray irradiation in this study. In the present study, the extent of cardiomyocyte damage caused by X-ray exposure was determined, alterations in oxidation/antioxidation levels were assessed, and changes in the expression of genes related to mitochondria were examined. The degree of myocardial tissue and cell injury was also determined. Dihydroethidium (DHE) staining, reactive oxygen species (ROS) assays, and glutathione (GSH) and manganese superoxide dismutase (Mn-SOD) assays were used to assess cell oxidation/antioxidation. Flow cytometry was used to determine the mitochondrial membrane potential and mitochondrial permeability transition pore (mPTP) opening. High-throughput transcriptome sequencing and bioinformatics analysis were used to elucidate the expression of mitochondria-related genes in myocardial tissue induced by X-ray exposure. Polymerase chain reaction (PCR) was used to verify the expression of differentially expressed genes.

Results: X-ray irradiation damaged myocardial tissue and cells, resulting in an imbalance of oxidative and antioxidant substances and mitochondrial damage. NAC treatment increased cell counting kit-8 (CCK-8) levels (P=0.02) and decreased lactate dehydrogenase (LDH) release (P=0.02) in cardiomyocytes. It also reduced the level of ROS (P=0.002) and increased the levels of GSH (P=0.04) and Mn-SOD (P=0.01). The mitochondrial membrane potential was restored (P<0.001), and mPTP opening was inhibited (P<0.001). Transcriptome sequencing and subsequent validation analyses revealed a decrease in the expression of mitochondria-related genes in myocardial tissue induced by X-ray exposure, but antioxidant therapy did not reverse the related DNA damage.

Conclusions: Antioxidants mitigated radiation-induced myocardial damage to a certain degree, but these agents did not reverse the associated DNA damage. These findings provide a new direction for future investigations by our research group, including exploring the treatment of RIHD-related DNA damage.

Keywords: Radiation-induced heart disease (RIHD); N-acetylcysteine (NAC); mitochondrial oxidative stress; mitochondrial DNA (mtDNA)

Submitted Jan 09, 2024. Accepted for publication Jul 11, 2024. Published online Aug 21, 2024.
doi: 10.21037/cdt-24-19
View this article at: https://dx.doi.org/10.21037/cdt-24-19

Introduction

Background

Radiation therapy is a crucial treatment method for tumors. With continuing improvements in patient survival rates, radiation-induced heart disease (RIHD) has emerged as a serious complication in thoracic cancer patients (1-3). The prevention and management of RIHD pose considerable clinical challenges due to the delayed onset of symptoms and its detrimental impact on long-term cancer survivors, which leads to diminished quality of life and increased health care expenditures (4,5).

Rationale and knowledge gap

The primary cause of RIHD is the excessive generation of reactive oxygen species (ROS) and reactive nitrogen species (RNS) that result from the substantial radiolytic decomposition of water within tissues and cells (6-8). The abundance of ROS directly damages subcellular organelles and exerts negative effects on various macromolecules, such as DNA, which is exacerbated by the limited availability of intracellular antioxidants (9,10). An imbalance in oxidation and antioxidant levels ensues, which triggers oxidative stress and further exacerbates RIHD. Therefore, oxidative stress has emerged as a prominent and important process in RIHD (7,11).

At present, antioxidants have become an important means of treating RIHD. Hesperidin, a natural antioxidant, can reduce radiation-induced cardiac damage. After hesperidin was administered to mice with radiation-induced heart damage, the oxidative stress level decreased significantly (12,13). Melatonin has been reported to suppress NF-κB-mediated signaling pathways and protect mitochondria from radiation-induced DNA damage, thereby mitigating oxidative stress. Farhood *et al.* reported that melatonin may also have a protective effect on heart damage caused by ionizing radiation by inhibiting the expression of interleukin-4, DUOX1, and DUOX2 (14,15). The above antioxidants require certain special conditions to exert their effects, especially the dosage and redox conditions in cells. For example, it has been shown that high concentrations of melatonin can induce excessive accumulation of intracellular ROS, play an upstream pro-oxidative role in mitochondria-mediated apoptosis and autophagy, and promote lipid peroxidation and/or induce DNA damage (16). N-acetylcysteine (NAC) is an important significant antioxidant that is widely used in clinical settings for the treatment of various diseases, such as bronchitis, acute respiratory distress syndrome, ischemia-reperfusion heart injury, and neuropsychiatric disorders (17).

Objective

The complexity and severity of RIHD limit clinical studies, and mouse models have played a central role in improving our understanding of the cardiac response to radiation. At present, rodent models of radiation-induced heart injury involve a wide range of radiation types and lesion latencies, which can objectively reflect cardiovascular changes in patients with thoracic malignant tumors after receiving radiotherapy (18). The present study evaluated the changes in oxidative stress and antioxidant levels in the cardiomyocytes of RIHD model rats and elucidated the expression patterns of mitochondria-related genes in RIHD model rats using high-throughput transcriptome sequencing. The impact of NAC intervention on RIHD was investigated to examine the potential benefits of antioxidant therapy. We present this article in accordance with the ARRIVE reporting checklist (available at https://cdt.amegroups.com/article/view/10.21037/cdt-24-19/rc).

Highlight box

Key findings
- N-acetylcysteine has therapeutic effects on radiation-induced heart disease (RIHD) due to its antioxidant activity.

What is known and what is new?
- It is known that X-rays induce oxidative stress in tissues.
- This study reveals the DNA damage of mitochondria-related genes in cardiomyocytes caused by X-rays.

What is the implication, and what should change now?
- We can consider antioxidant therapy and the repair of mitochondrial damage as potential directions for the treatment of RIHD.

Methods

Animal feeding and construction of the RIHD animal model

The present study used 8-week-old male Sprague-Dawley (SD) rats as experimental animals. Rats were purchased from the Research and Experimental Center of Gansu University of Chinese Medicine. The rats were housed in cages under controlled temperatures (22 to 24 ℃) and a 12 hours light/12 hours dark cycle with three to five rats per cage and given adequate feed and water. The model was established after 1 week of adaptation to the standard diet. The rats were randomly divided into two groups, a control group and an irradiation group (10 animals/group). The experimental mice were grouped using a random number table. During modeling, the rats were anesthetized via the intraperitoneal administration of 1% sodium pentobarbital, and only the heart was exposed to X-ray radiation by shielding the rats with a homemade lead brick. A small animal irradiator (model No. 225, Precision X-ray Inc., Madison, CT, USA) was used to deliver a 25 Gy X-ray dose to the heart. The following instrument parameters were used: voltage 225 kV, current 13.3 mA, irradiation distance 48 cm source-to-surface distance, and dose rate 2 Gy/min. The final dose of 25 Gy was administered to the experimental animals after the dose rate (2 Gy/min) was determined. For example, we prespecified a total dose of 25 Gy to be delivered to the animal, and a one-time 12.5-minute irradiation period was determined based on the dose rate calculation. After irradiation, the rats received a regular diet. A total of two animals in the irradiated group died during feeding after irradiation. It may be caused by heart failure. After 12 weeks of feeding, the orbital blood of the rats was collected after intraperitoneal anesthesia, the myocardial tissue was collected for lavage, and the blood and myocardial tissue samples were analyzed. The success of the animal model was evaluated by detecting the serum levels of creatine kinase-MB (CK-MB) and lactate dehydrogenase (LDH). The isolated samples were rapidly placed in liquid nitrogen and stored at −80 ℃ until the experiments were performed. The experiments were performed under a project license (No. 2023-224) granted by the ethics board of Gansu Provincial Hospital, in compliance with national guidelines for the care and use of animals. Finally, animal carcasses were sealed in special plastic bags, collected and stored in prescribed freezers for regular processing by the commissioner. A protocol was prepared before the study without registration.

Cell culture and the RIHD cell model

The H9C2 cell line was kindly provided by the Cell Bank of the Chinese Academy of Sciences. Complete medium was prepared with Dulbecco's modified Eagle medium (DMEM; Basal Media, Shanghai, China), 10% fetal bovine serum (ABWbio, Uruguay), and 1% double antibiotics (100 U/mL penicillin + 100 mg/mL streptomycin, cat. S110JV, Basal Media). The cells were cultured in a constant temperature incubator at 37 ℃ with 5% CO_2. To establish the model, cells were placed in culture flasks or dishes and directly irradiated using a small animal irradiator. The irradiation method used for the cells was the same as that used for the animal model. For example, we applied an irradiation dose of 8 Gy to the cells using a one-time irradiation period of 4 minutes based on the dose rate calculation. The complete medium was immediately replaced at the end of irradiation, and the cells were treated with NAC (10 μM). The model was successfully established and used for experiments after continuing conventional culture for 48 hours. The success of the cell modeling was evaluated by assessing cell viability using a cell counting kit-8 (CCK-8) assay and determining LDH levels. Initially, H9C2 cells were exposed to varying doses of radiation (0, 4, 8 and 12 Gy) to elucidate the impact of radiation, and 8 Gy was selected as the irradiation dose for subsequent studies of cardiomyocytes and NAC intervention. To clarify the effect of NAC on radiation-damaged cardiomyocytes, cells were treated with low (5 μM) and high (10 μM) doses of NAC. The high dose was subsequently determined as the cell administration dose.

Transmission electron microscopy (TEM)

The myocardial tissue was fixed overnight at room temperature using a 3% glutaraldehyde electron microscope fixative. Next, the sample was fixed in cacodylate buffer containing 1% OsO_4 at 4 ℃ for 2 hours. The samples were gradually dehydrated using ethanol and propylene oxide. The tissue samples were sectioned after agarose gel polymerization and affixed onto a slit grid coated with polyformaldehyde. For electron microscopy samples, staining was performed using uranyl acetate and lead citrate. TEM (Talos F200C, 200 kV, FEI, Hillsborough, OR, USA) was used to capture images of each group of samples.

Dihydroethidium (DHE) staining

The myocardial tissue was promptly immersed in liquid

Table 1 Primer sequence

Gene	Forward primer (5'→3')	Reverse primer (5'→3')
β-actin	TTGACATCCGTAAAGACC	ATAGAGCCACCAATCCA
Ndufa6	CACACATTATGCGGTTCTTC	GGGTCATGGCCAATATAGAA
Mrps14	AGTTGTGAGGAACCAACATT	AGCAACTCATTTACTCTGAACA
Mt-co3	GGATTTCATGGCCTCCACGTA	TCATGCTGCGGCTTCAAATC
Mff	TTGGTCAGAAACGATTCCAT	TAGCACGCTCTTTATTCTCC
Park7	TGGCTCACGAAGTAGGCTTT	GCTGTAGTGACTGCCGTTC

nitrogen following *in vitro* lavage, and frozen sections were prepared. The frozen sections were immersed in phosphate-buffered saline (PBS) and washed via three rounds of shaking on a shaker. Each section was treated with an appropriate quantity of DHE staining reagent (cat. S0063, Beyotime Biotechnology, Shanghai, China) and incubated at 37 ℃ for 30 minutes in the dark. The tissue sections were washed three times with PBS. The sections were incubated with 4',6-diamidino-2-phenylindole (DAPI) at room temperature for 10 minutes. A fluorescence quencher was used to seal the film. Image acquisition and analysis were performed.

Blood analysis

Blood samples were obtained from the rats prior to sacrifice. The collected blood was incubated at room temperature for 4 hours before centrifugation to obtain the serum. An automatic biochemical instrument was used analyze the blood parameters, and the determination of CK-MB and LDH levels was meticulously performed in accordance with the provided instructions. The acquired data were exported for further analyses.

RNA sequencing (RNA-seq) and bioinformatics analysis

Transcriptome sequencing was performed on myocardial tissues from SD rats. The animals were randomly divided into a control group and a radiation group. The raw files of high-throughput sequencing were converted to the original sequences. Quality control was conducted to obtain high-quality sequences suitable for downstream data analysis. The raw data were filtered to remove reads that did not meet the analysis criteria to obtain clean reads for subsequent analyses, and the clean reads were aligned with the reference genome sequence. The messenger RNA (mRNA) expression levels were normalized for comparisons between different samples. The limma package in R was used to compare the differences between biological replicates, and the edgeR package was used for comparisons of samples without biological replicates. The following standards were used for the differential expression of mRNAs: $|\log_2\text{fold change}| \geq 1$ and P value ≤0.05 or less. Gene Ontology (GO) and Kyoto Encyclopedia of Genes and Genomes (KEGG) enrichment analyses were performed. The raw sequence data reported in this paper have been deposited in the Genome Sequence Archive (Genomics, Proteomics & Bioinformatics 2021) of the National Genomics Data Center (Nucleic Acids Res 2022), China National Center for Bioinformation/Beijing Institute of Genomics, Chinese Academy of Sciences (GSA: CRA014164), which are publicly accessible at https://ngdc.cncb.ac.cn/gsa.

RNA isolation and reverse transcription-quantitative polymerase chain reaction (RT-qPCR) analysis

After the RNA-degrading enzymes in the samples were removed with isopropyl alcohol, total RNA was extracted from the cells using TRIzol reagent (cat. 15596018, Invitrogen, Ambion, Carlsbad, CA, USA). The concentration of extracted RNA was determined using a nucleic acid analyzer. The extracted RNA was reverse transcribed into cDNA using a reverse transcription kit (cat. CW2019M, CWBIO, Taizhou, China). Specific primers for *β-actin*, *Ndufa6*, *Mrps14*, *Mt-co3*, *Mff*, and *Park7* were designed using Primer 5.0 software (*Table 1*). The relative expression levels of *Ndufa6*, *Mrps14*, *Mt-co3*, *Mff*, and *Park7* were detected using amplification kits. *β-actin* was used as a reference gene.

Cell viability assay

Cell viability was determined using a CCK-8 (cat. M4839,

Abmole, Houston, TX, USA). The cells were cultured in 96-well plates (5,000 cells/well) for 1 day. The plates were irradiated with a small animal irradiator and then cultured at 37 ℃ for 48 hours. The detection reagent was added, and the absorbance at 450 nm was measured using a microplate reader.

LDH release assay

LDH reflects the degree of myocardial cell injury. The cell culture medium was collected at the end of treatment, and the supernatant was collected after centrifugation. The relevant reaction reagents were added to the 96-well plate in strict accordance with the manufacturer's instructions (cat. A020-2-2, Nanjing Jiancheng Bioengineering Institute, Nanjing, China), and the absorbance at 450 nm was measured.

Determination of glutathione (GSH) and manganese superoxide dismutase (Mn-SOD) levels

Forty-eight hours after irradiation, the cells in each group were collected and sonicated. The supernatant was collected for subsequent detection after centrifugation. The corresponding reagents were added in strict accordance with the manufacturer's instructions for GSH (cat. BC1175, Beijing Solarbio Science & Technology, Beijing, China) and Mn-SOD (cat. S0103, Beyotime Biotechnology) analyses. The absorbance at 412 and 450 nm was measured using a microplate reader.

Flow cytometry analysis

Flow cytometry was used to assess the presence of ROS (cat. E004-1-1, Nanjing Jiancheng Bioengineering Institute), the mitochondrial membrane potential (JC-1, cat. C2003S, Beyotime Biotechnology), and mitochondrial permeability transition pore (mPTP) opening (cat. C2009S, Beyotime Biotechnology). After the establishment of the radiation cardiomyocyte model, H9C2 cells were suspended in liquid medium containing DCFH-DA, JC-1, and calcein AM fluorescent probes and incubated at 37 ℃ in a 5% CO_2 incubator for 30 minutes. The data were obtained using flow cytometry.

Statistical analyses

GraphPad Prism software (version 8.0) was used for the statistical analyses. The results are presented as the mean ± standard deviation. The statistical significance of all datasets was analyzed using analysis of variance (ANOVA). A 95% confidence interval was used, and $P<0.05$ indicated statistical significance (two-sided test).

Results

X-rays induce myocardial injury and oxidative stress in rats

TEM analysis of myocardial tissue samples from rats with RIHD revealed mitochondrial edema and a rounded mitochondrial morphology. We observed partial disruption of mitochondrial integrity, a blurred mitochondrial membrane, and significant reduction and fragmentation of mitochondrial cristae (*Figure 1A*). Analysis of serum biochemical markers revealed a significant increase in the levels of CK-MB and LDH, which are indicators of myocardial injury (*Figure 1B*,*1C*, $P<0.001$). The fluorescent probe DHE is frequently used to determine the concentration of superoxide anions. DHE staining revealed a noticeable increase in red staining localized in the nucleus and cytoplasm in the myocardial tissue of the model group (*Figure 1D*,*1E*, $P=0.048$). These findings indicate that X-ray exposure produced myocardial injury and elevated the levels of ROS.

X-rays induce myocardial cell damage

The CCK-8 assay results suggested that cell viability gradually decreased in a dose-dependent manner in the radiation groups compared to the control group ($P<0.001$), which indicated that radiation inhibited the viability of myocardial cells (*Figure 2A*). LDH, which is another indicator used to characterize the degree of cell damage, increased with increasing radiation dose ($P=0.02$), as shown in *Figure 2B*. The results of the CCK-8 and LDH assays were consistent and indicated that radiation-induced myocardial cell injury was dose-dependent.

X-ray irradiation induces oxidative stress in cardiomyocytes

ROS is the most direct indicator of oxidative stress in cells. GSH and SOD are important antioxidant substances, and Mn-SOD is the isoform of SOD in mitochondria. Flow cytometry showed that the ROS level gradually increased with increasing radiation dose

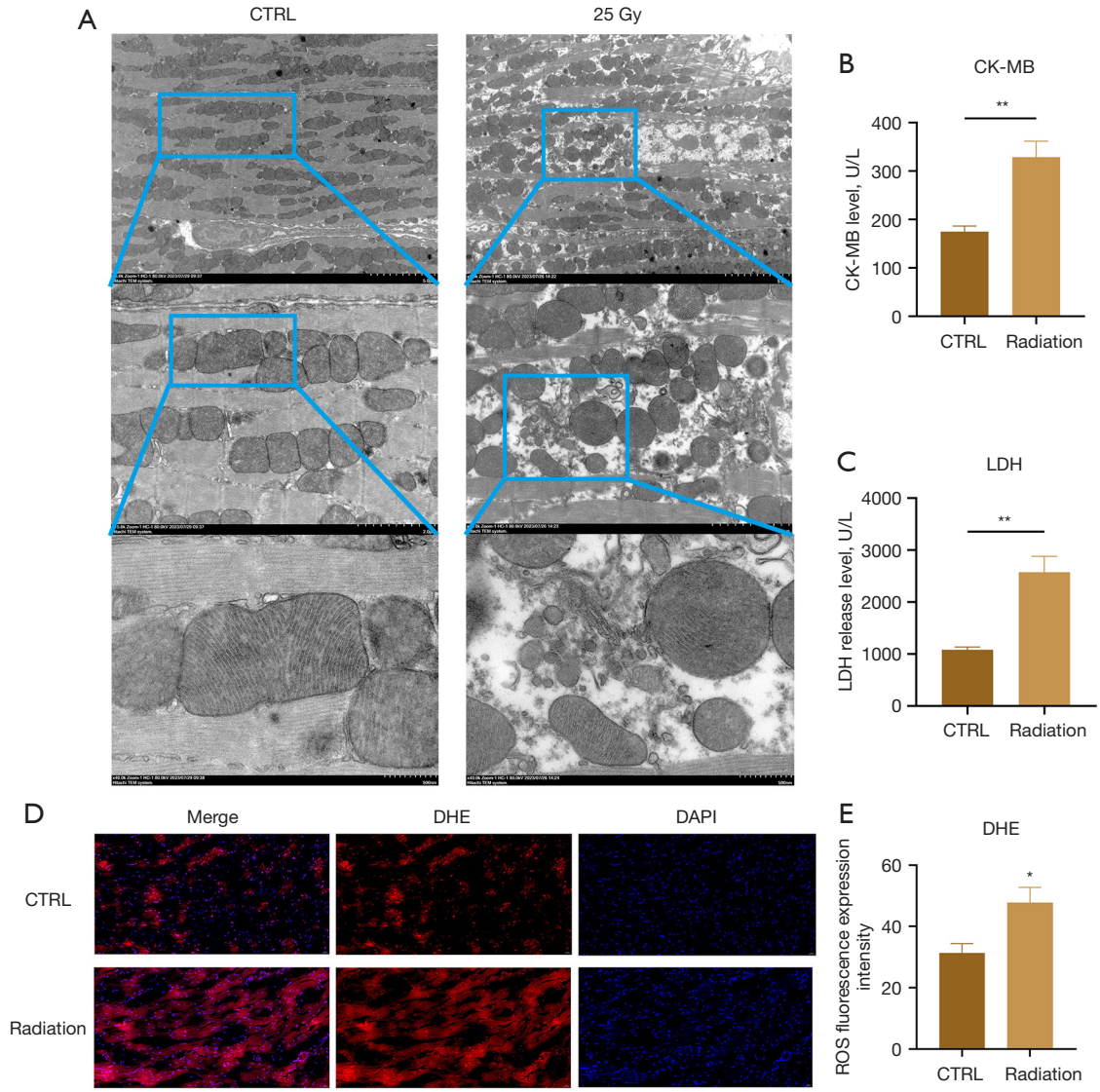

Figure 1 Effect of X-rays on the rat heart. (A) The ventricular tissue was observed by TEM. The magnification is respectively ×5,000, ×15,000 and ×40,000. (B,C) Serum samples were collected to observe changes in cardiac injury indicators. (D,E) Changes in ROS production in the myocardial tissue of the rats were observed. The magnification is respectively ×400. n≥3. *, compared with control group P<0.05; **, compared with control group P<0.01. CTRL, control group; CK-MB, creatine kinase-MB; LDH, lactate dehydrogenase; DHE, dihydroethidium; DAPI, 4',6-diamidino-2-phenylindole; ROS, reactive oxygen species; TEM, transmission electron microscopy.

(P=0.02). This indicated that ROS were produced by radiation-exposed cardiomyocytes (*Figure 3A,3B*). The level of Mn-SOD (P=0.02) gradually decreased with increasing radiation dose. Although the decrease in GSH levels (P=0.009) was not significant, it still exhibited a downward trend. These results indicated that radiation affected the antioxidant capacity of cardiomyocytes (*Figure 3C,3D*).

X-ray irradiation induces mitochondrial damage in myocardial cells

The decreased mitochondrial membrane potential in damaged cells inhibits the accumulation of JC-1 in the mitochondrial matrix and generates green fluorescence. A significant increase in green fluorescence intensity was observed in myocardial cells exposed to increasing radiation

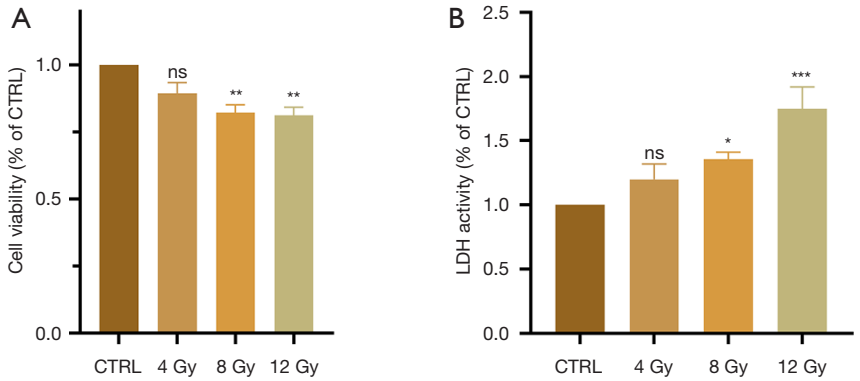

Figure 2 Effect of X-ray irradiation on cardiomyocyte viability and LDH levels. (A) Results of the cell viability assay. (B) Results of the measurement of LDH release. n≥3. *, compared with control group P<0.05; **, compared with control group P<0.01; ***, compared with control group P<0.001; ns, not statistically. CTRL, control group; LDH, lactate dehydrogenase.

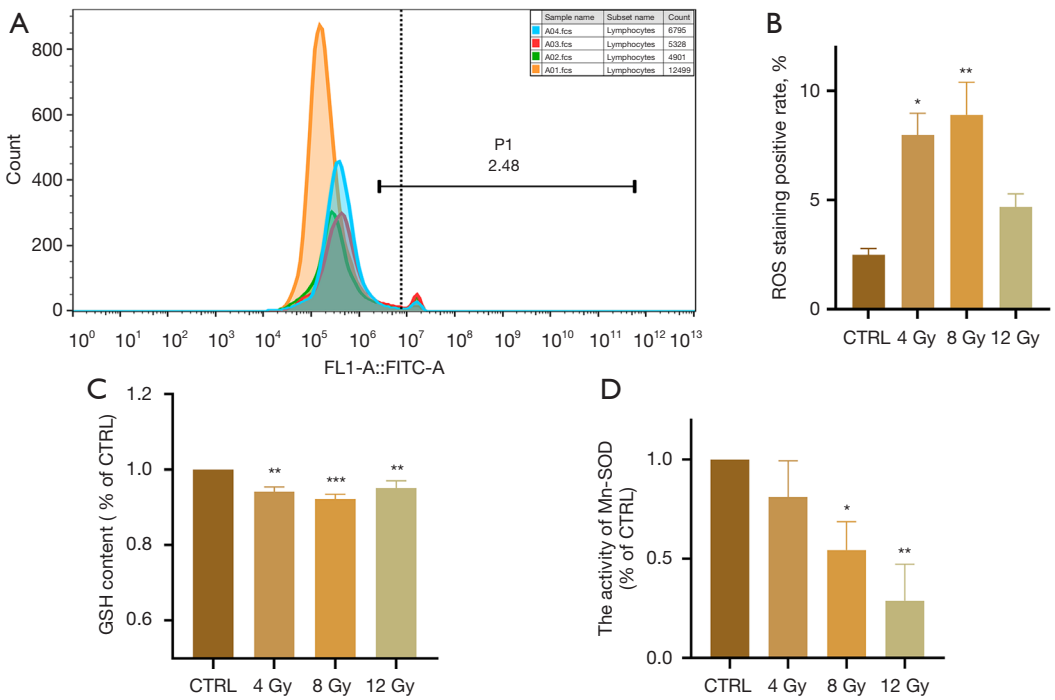

Figure 3 Effect of X-rays on the oxidative capacity of cardiomyocytes. (A) ROS levels were determined by flow cytometry. (B) Statistical analysis of the ROS levels. (C) GSH levels. (D) Results of the Mn-SOD activity assay. n≥3. *, compared with control group P<0.05; **, compared with control group P<0.01; ***, compared with control group P<0.001. CTRL, control group; ROS, reactive oxygen species; GSH, glutathione; Mn-SOD, manganese superoxide dismutase.

doses, which indicated a decrease in the mitochondrial membrane potential (*Figure 4A,4B*) (P<0.001). The opening of the mPTP is a crucial event that leads to cell death and plays a vital role in modulating cell survival and apoptosis. The extent of mitochondrial mPTP opening was assessed based on the intensity of green fluorescence within the mitochondria, and a decrease in green fluorescence intensity corresponds to a greater degree of opening. Our results demonstrated a reduction in green fluorescence intensity with increasing radiation dose, which indicated a dose-dependent relationship between mPTP opening and radiation dose (*Figure 4C,4D*) (P<0.001).

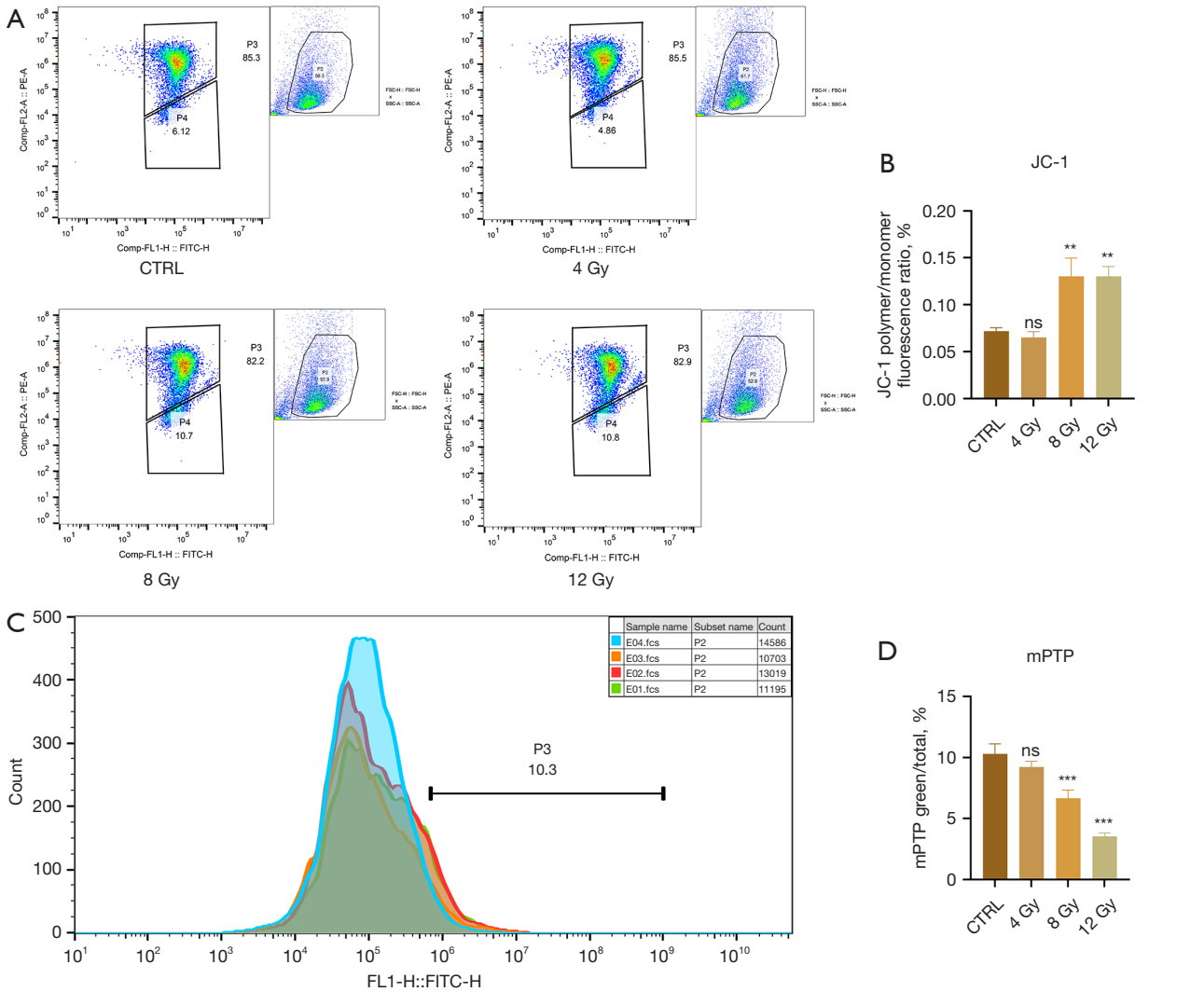

Figure 4 Effect of X-rays on the mitochondria of cardiomyocytes. (A,B) Mitochondrial membrane potential was detected by flow cytometry. (C,D) mPTP opening was detected by flow cytometry. n≥3. **, compared with control group P<0.01; ***, compared with control group P<0.001; ns, not statistically. CTRL, control group; mPTP, mitochondrial permeability transition pore.

Differential expression of mitochondria-related genes in RIHD model rats

Transcriptome sequencing and bioinformatics analysis revealed 876 differentially expressed genes between the radiation group and the control group, of which 466 and 410 genes were upregulated and downregulated, respectively (*Figure 5A-5C*). After comparing the differentially expressed genes obtained by sequencing with the data in the mitochondrial gene database (https://www.broadinstitute.org/), 26 mitochondria-related genes were found, including 11 upregulated and 15 downregulated genes, as shown in *Table 2* and *Figure 5D-5F*. GO analysis (*Figure 5G*) revealed that the biological processes enriched in these 26 genes included those related to mitochondrial structure and lipopolysaccharide stimulation, hypoxia induced by hydrogen peroxide, and drug regulation in biological processes. The enriched cellular components in these genes included components of the cell membrane. Molecular function (MF) analysis revealed that these genes were primarily involved in protein synthesis. KEGG enrichment analysis (*Figure 5H*) revealed that the metabolic pathway of amino acids was primarily enriched in these genes, and these results demonstrated the effects of X-rays

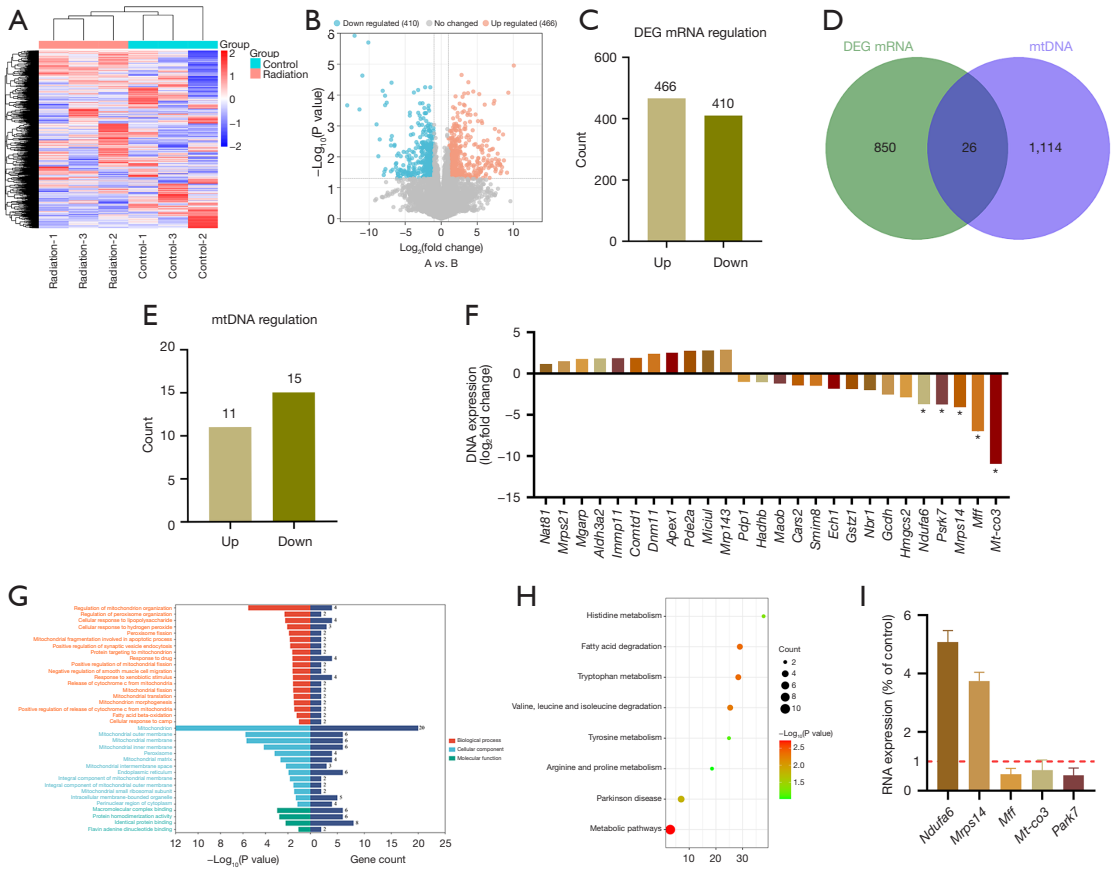

Figure 5 Results of transcriptome sequencing, bioinformatics analysis and experimental verification. (A,B) Heatmap and volcano plot of the transcriptome sequencing results. (C) Number of upregulated and downregulated DEGs. (D) Shared DEGs and mitochondria-related genes. (E) Number of upregulated and downregulated mitochondria-related genes. (F) Expression of 26 differentially expressed mitochondria-related genes. (G) Histogram of GO enrichment analysis results. (H) Bubble map of the KEGG enrichment analysis results. (I) Expression of DEGs. The red line indicated the relative expression of genes in normal cells. *, represents mitochondria-related genes with the most significant differential expression. DEG, differentially expressed gene; mRNA, messenger RNA; mtDNA, mitochondrial DNA; GO, Gene Ontology; KEGG, Kyoto Encyclopedia of Genes and Genomes.

on the energy metabolism function of mitochondria.

We selected five of the 26 genes with the highest significance for expression verification. Notably, these genes were all downregulated (*Figure 5F*). PCR revealed that the expression of *Ndufa6* and *Mrps14* increased, which contradicted the sequencing results, and the expression of *Mff*, *Mt-co3*, and *Park7* decreased, which was consistent with the sequencing results (*Figure 5I*).

NAC inhibits radiation-induced myocardial cell injury

NAC is a well-known antioxidant, and we examined its effects on radiation-induced oxidation as a potential treatment for RIHD. We treated irradiated H9C2 cells with different doses of NAC. CCK-8 assay results showed no significant difference in the low-dose (5 μM) group, but cell viability gradually increased with increasing NAC concentrations (10 μM) (P=0.02) (*Figure 6A*). Subsequent experiments revealed that NAC reduced the release of LDH in cardiomyocytes induced by radiation-induced heart injury (P=0.02) (*Figure 6B*). Therefore, NAC has a certain anti-injury effect on RIHD.

NAC inhibits radiation-induced oxidative stress in cardiomyocytes

To further clarify the effect of NAC on radiation-induced oxidative stress in cardiomyocytes, changes in ROS levels

Table 2 Differential expression of mitochondria-related genes

Symbol	Regulation	Log_2FC	P value	Description
Ndufa6†	Down	–3.7001	0.02	NADH: ubiquinone oxidoreductase subunit A6
Mrpl43	Up	2.901	0.03	Mitochondrial ribosomal protein L43
Mrps14†	Down	–4.050	0.01	Mitochondrial ribosomal protein S14
Ech1	Down	–1.828	0.040	Enoyl-CoA hydratase 1
Mrps21	Up	1.485	0.01	Mitochondrial ribosomal protein S21
Gcdh	Down	–2.534	0.045	Glutaryl-CoA dehydrogenase
Cars2	Down	–1.418	0.004	Cysteinyl-tRNA synthetase 2, mitochondrial
Immp1l	Up	1.856	0.047	Inner mitochondrial membrane peptidase subunit 1
Hmgcs2	Down	–2.860	0.005	3-hydroxy-3-methylglutaryl-CoA synthase 2
Gstz1	Down	–1.859	0.02	Glutathione S-transferase zeta 1
Pdp1	Down	–1.010	0.007	Pyruvate dehydrogenase phosphatase catalytic subunit 1
Hadhb	Down	–1.044	0.049	Hydroxyacyl-CoA dehydrogenase trifunctional multienzyme complex subunit beta
Aldh3a2	Up	1.839	0.005	Aldehyde dehydrogenase 3 family, member A2
Mt-co3†	Down	–10.941	2.35	Mitochondrially encoded cytochrome c oxidase III
Dnm1l	Up	2.393	0.02	Dynamin 1-like
Micu1	Up	2.817	2.24	Mitochondrial calcium uptake 1
Smim8	Down	–1.476	0.03	Small integral membrane protein 8
Maob	Down	–1.185	0.006	Monoamine oxidase B
Mff†	Down	–6.980	0.004	Mitochondrial fission factor-like
Park7†	Down	–3.731	0.03	Parkinsonism associated deglycase
Mgarp	Up	1.768	0.041	Mitochondria-localized glutamic acid-rich protein
Comtd1	Up	1.888	0.02	Catechol-O-methyltransferase domain containing 1
Apex1	Up	2.519	0.001	Apurinic/apyrimidinic endodeoxyribonuclease 1
Nbr1	Down	–2.001	0.006	NBR1, autophagy cargo receptor
Pde2a	Up	2.754	0.02	Phosphodiesterase 2A
Nat8l	Up	1.183	0.01	N-acetyltransferase 8-like

†, represents the target gene with the highest significance. FC, fold change.

were determined using flow cytometry. When NAC was administered, the ROS levels in H9C2 cells after irradiation decreased significantly compared to those in the irradiation group (P=0.002) (*Figure 7A*,*7B*). Moreover, the levels of GSH (P=0.04) and Mn-SOD (P=0.01) in the irradiated cells treated with NAC were higher than those in the irradiated group (*Figure 7C*,*7D*). These results indicate that NAC reduced ROS levels and restored the antioxidant capacity of irradiated cells.

NAC alleviates radiation-induced myocardial mitochondrial damage

Our findings indicated that treatment with the antioxidant NAC effectively restored the mitochondrial membrane potential of irradiated cardiomyocytes (P<0.001). There was a notable increase in green fluorescence intensity during mPTP detection, which indicated a significant decrease in the degree of mPTP opening (P<0.001), as

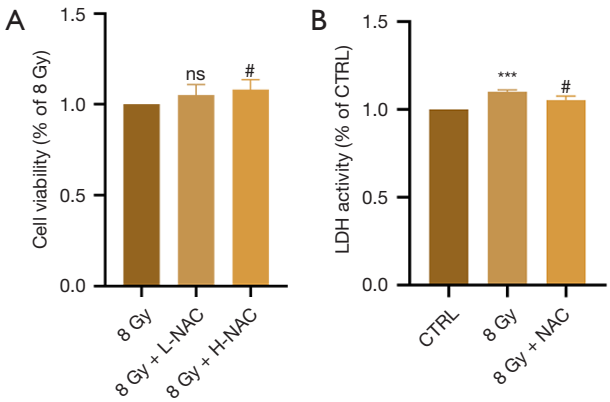

Figure 6 Effect of NAC on RIHD. (A) Results of the cell viability assay. (B) Results of the measurement of LDH release. n≥3. #, compared with 8 Gy group P<0.05; ***, compared with control group P<0.001; ns, not statistically. CTRL, control group; L-NAC, 5 μM, low-NAC; NAC, N-acetylcysteine; H-NAC, 10 μM, high-NAC; LDH, lactate dehydrogenase; RIHD, radiation-induced heart disease.

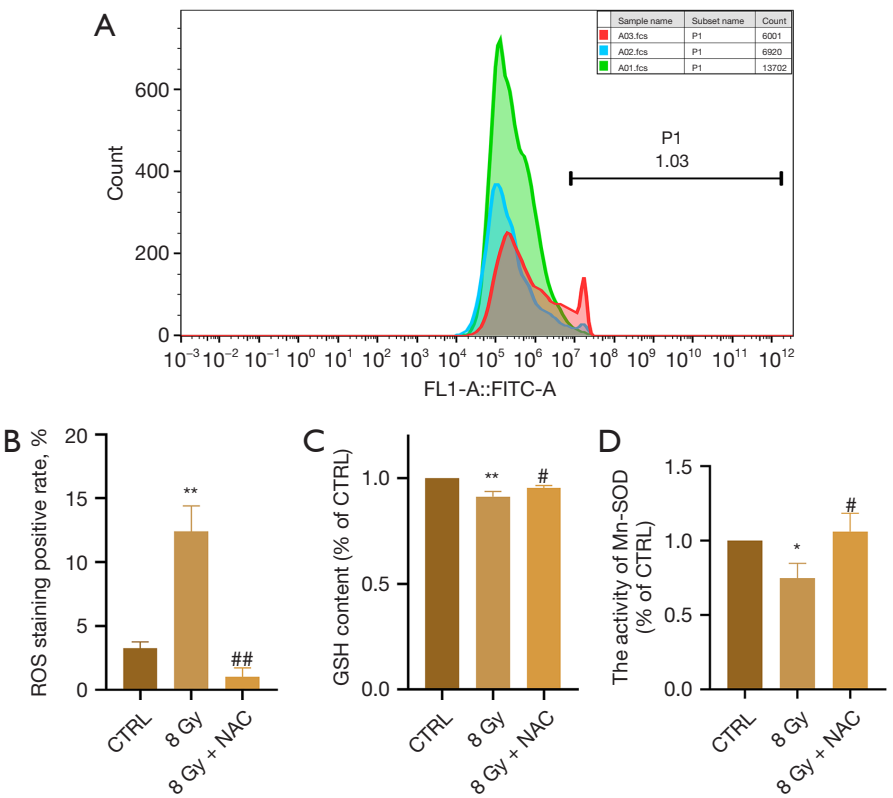

Figure 7 Effect of NAC on RIHD induced oxidative stress. (A) ROS levels were measured by flow cytometry. (B) Statistical analysis of the ROS levels. (C) GSH levels. (D) Results of the Mn-SOD activity assay. n≥3. #, compared with 8 Gy group P<0.05; ##, compared with 8 Gy group P<0.01; *, compared with control group P<0.05; **, compared with control group P<0.01. CTRL, control group; ROS, reactive oxygen species; NAC, N-acetylcysteine; GSH, glutathione; Mn-SOD, manganese superoxide dismutase; RIHD, radiation-induced heart disease.

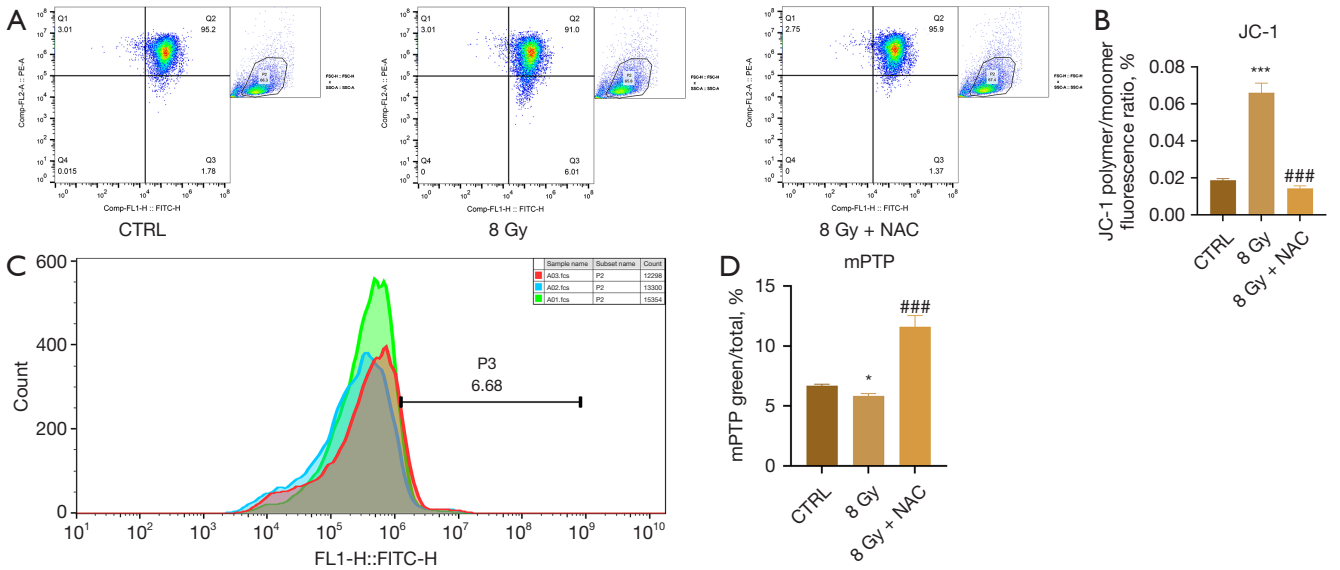

Figure 8 Effect of NAC on X-ray induced mitochondrial damage in cardiomyocytes. (A,B) Mitochondrial membrane potential was detected by flow cytometry. (C,D) mPTP opening was detected by flow cytometry. n≥3. ###, compared with 8 Gy group P<0.001; *, compared with control group P<0.05; ***, compared with control group P<0.001. CTRL, control group; NAC, N-acetylcysteine; mPTP, mitochondrial permeability transition pore.

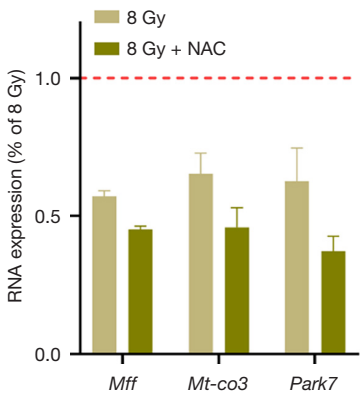

Figure 9 Effect of NAC on the abnormal expression of mitochondria-related genes induced by RIHD. The expression of each gene was verified by PCR. The red line indicated the relative expression of genes in normal cells. NAC, N-acetylcysteine; RIHD, radiation-induced heart disease; PCR, polymerase chain reaction.

shown in *Figure 8A-8D*.

NAC does not ameliorate radiation-induced mitochondrial-related gene damage

We investigated whether antioxidant intervention could abrogate the abnormal expression of mitochondria-related proteins in radiation-induced myocardial injury. After NAC treatment, the expression levels of *Mff*, *Mt-co3*, and *Park7* were determined via PCR. The results showed that NAC did not increase the expression of these genes compared with that in the radiation group and even showed a further downward trend (P<0.05) (*Figure 9*).

Discussion

Key findings

The oxidant and antioxidant systems normally maintain a dynamic balance in the body, which is crucial for numerous metabolic processes. The primary factors contributing to oxidative stress injury in RIHD are the generation of ROS and RNS via several mechanisms, such as direct hydrolysis of water by radiation, disruption of the respiratory chain, and substantial depletion of antioxidants that cannot be adequately restored (8,19-22). The resultant oxidative stress exacerbates cellular deterioration. Excessive consumption of the intracellular antioxidant GSH is a contributing factor to oxidative stress. SODs are a family of enzymes with antioxidant properties that are categorized into cuprum (Cu)/zinc (Zn)-SODs and Mn-SODs (23). Mn-SOD is predominantly localized in mitochondria, where it plays

a crucial role in safeguarding mitochondria against free radical-induced harm due to its involvement in energy production and aerobic metabolism (24). Therefore, Mn-SOD has garnered increasing scientific research interest. We confirmed that X-rays induced excessive ROS production in cardiomyocytes. The levels of GSH and Mn-SOD decreased following radiation, which indicated that radiation therapy disrupted the equilibrium between oxidation and antioxidation within cardiomyocytes to promote oxidative stress-induced harm.

Mitochondria are important for the generation of ROS (25-28). Mitochondrial ROS, particularly under pathological conditions, negatively affect a range of cellular components, including mitochondrial DNA (mtDNA), biofilms, and diverse proteins (29). The mPTP is located at the interface of the outer and inner mitochondrial membranes (30). The opening of the mPTP is widely regarded as an indicator of cell death, and it serves as a pivotal mechanism that initiates the progression of various pathologies and organ disorders (31). The induction of mPTP opening is primarily attributed to the flow of Ca^{2+}, with ROS production and reduced mitochondrial membrane potential acting as additional inducers (32,33). Cells experiencing heightened levels of oxidative stress exhibit pronounced susceptibility to the opening of the mPTP, which ultimately results in cell death (34). A decrease in the mitochondrial membrane potential and opening of the mPTP were observed in our RIHD experiments, and a certain degree of dependence on the X-ray dose was observed. In conclusion, X-ray exposure likely leads to the generation of ROS and subsequent damage to myocardial mitochondria.

NAC has been shown to play a primary role in various studies as a mucolytic agent and antidote against paracetamol overdose (35,36). Moreover, NAC can directly scavenge superoxide and peroxides, which safeguards cells from oxidative harm (37). Previous studies have also demonstrated the ability of NAC to withstand external oxidants (37-39). Some researchers have proposed that GSH synthesis is necessary to replenish GSH levels following oxidative stress, with Cys being a crucial substrate for GSH synthesis (40). In this context, NAC, as a precursor of Cys, may assist in the restoration of GSH levels subsequent to its depletion (41,42). GSH functions as a robust cellular antioxidant that proficiently counteracts excessive ROS to restore the balance between oxidative and antioxidant mechanisms within cellular systems. In the present study, the administration of NAC significantly increased intracellular GSH levels, which was accompanied by a notable reduction in ROS levels. Cellular viability was also partially restored, and cellular injury was mitigated to a certain extent. When intracellular oxidative stress was corrected by NAC, the function of mitochondria in myocardial cells was restored. These findings suggest that NAC exhibits antioxidant properties and may have therapeutic value in the management of radiation-induced injuries.

Strengths and limitations

It is indisputable that radiation directly or indirectly damages DNA, which leads to cellular senescence and may trigger apoptosis (43,44). In apolipoprotein E knockout mice, exposure to 6 Gy irradiation increased the expression of DNA damage markers (γ-H2AX and 53BP1) and accelerated plaque growth and the development of atherosclerosis (45). Another *in vitro* study demonstrated that the exposure of human umbilical vein endothelial cells to 4 Gy of radiation led to the activation of ATM, CHK2, p53/p21, and other factors linked to senescence (46). The presence of radiation-induced DNA damage was detected. Cardiac endothelial cells exhibit strong inflammatory responses and increased expression of the DNA damage response protein DDB2 when exposed to high doses of gamma rays (10 Gy) (47). Most intracellular ROS originate from mitochondria and strongly influence the intracellular equilibrium between oxidative stress and antioxidant defense mechanisms in the event of mitochondrial impairment. In the present study of the influence of X-ray-induced heart injury on mitochondria-related genes, the expression levels of three specific genes, namely, *Mff*, *Mt-co3*, and *Park7*, were decreased. Despite the administration of an antioxidant, there was no significant increase in the expression of these genes. Therefore, we hypothesized that treatment with antioxidants, particularly NAC, may not effectively reverse radiation-induced mtDNA damage. Notably, although antioxidant treatment offers transient protection against radiation-induced oxidative stress, it fails to address underlying and enduring damage, such as DNA damage. It is very difficult to obtain myocardial tissue from clinical patients. In addition, RIHD animal and cell models cannot 100% simulate the situation of tumor patients after radiotherapy, which prevents us from obtaining reliable evidence.

Comparison with similar research

Recent studies have shown that NAC has a strong

antioxidant effect on various radiation-induced injuries. For example, NAC has therapeutic effects on X-ray-induced islet cell damage (48). NAC had a protective effect on radiation-induced oral mucositis both *in vivo* and *in vitro* (49). NAC also has a protective effect on radiation-induced renal injury in rats (50).

Explanations of findings

The findings of our study indicate that NAC has the potential to abrogate the decrease in GSH and Mn-SOD levels caused by RIHD, reduce the levels of ROS, and increase cell viability while mitigating cellular damage. Previous studies and the results of our research show that the strong antioxidant capacity of NAC has a potential therapeutic effect on RIHD, which is primarily caused by oxidative stress.

Conclusions

Notably, NAC has been used as an antioxidant in the treatment of lung diseases for many years in clinical practice with a certain degree of recognition, which provides reliability for further exploration of therapeutic drugs for RIHD. Further examination of the association between antioxidant therapy and DNA damage in RIHD may present novel opportunities for future research endeavors by our team and other scholars who are interested in this topic.

Acknowledgments

Funding: This work was supported by grants from the Natural Science Foundation of Gansu Province (No. 22JR5RA665), the Natural Science Foundation of Gansu Province (No. 20YF3WA011), the Scientific Research Fund Project of Gansu Provincial Hospital (No. ZX-62000001-2023-274), and the Innovation and Entrepreneurship Talent Project of Lanzhou (No. 2018-RC-72).

Footnote

Reporting Checklist: The authors have completed the ARRIVE reporting checklist. Available at https://cdt.amegroups.com/article/view/10.21037/cdt-24-19/rc

Data Sharing Statement: Available at https://cdt.amegroups.com/article/view/10.21037/cdt-24-19/dss

Peer Review File: Available at https://cdt.amegroups.com/article/view/10.21037/cdt-24-19/prf

Conflicts of Interest: All authors have completed the ICMJE uniform disclosure form (available at https://cdt.amegroups.com/article/view/10.21037/cdt-24-19/coif). The authors have no conflicts of interest to declare.

Ethical Statement: The authors are accountable for all aspects of the work in ensuring that questions related to the accuracy or integrity of any part of the work are appropriately investigated and resolved. The experiments were performed under a project license (No. 2023-224) granted by the ethics board of Gansu Provincial Hospital, in compliance with national guidelines for the care and use of animals.

References

1. Belzile-Dugas E, Eisenberg MJ. Radiation-Induced Cardiovascular Disease: Review of an Underrecognized Pathology. J Am Heart Assoc 2021;10:e021686.
2. Wang KX, Ye C, Yang X, et al. New Insights into the Understanding of Mechanisms of Radiation-Induced Heart Disease. Curr Treat Options Oncol 2023;24:12-29.
3. Quintero-Martinez JA, Cordova-Madera SN, Villarraga HR. Radiation-Induced Heart Disease. J Clin Med 2021;11:146.
4. van Nimwegen FA, Schaapveld M, Janus CP, et al. Cardiovascular disease after Hodgkin lymphoma treatment: 40-year disease risk. JAMA Intern Med 2015;175:1007-17.
5. Cheng YJ, Nie XY, Ji CC, et al. Long-Term Cardiovascular Risk After Radiotherapy in Women With Breast Cancer. J Am Heart Assoc 2017;6:e005633.
6. Ping Z, Peng Y, Lang H, et al. Oxidative Stress in Radiation-Induced Cardiotoxicity. Oxid Med Cell Longev 2020;2020:3579143.

7. Wang H, Wei J, Zheng Q, et al. Radiation-induced heart disease: a review of classification, mechanism and prevention. Int J Biol Sci 2019;15:2128-38.
8. Tapio S. Pathology and biology of radiation-induced cardiac disease. J Radiat Res 2016;57:439-48.
9. Bakshi MV, Barjaktarovic Z, Azimzadeh O, et al. Long-term effects of acute low-dose ionizing radiation on the neonatal mouse heart: a proteomic study. Radiat Environ Biophys 2013;52:451-61.
10. Wang G, Ma L, Wang B, et al. Tanshinone IIA Accomplished Protection against Radiation-Induced Cardiomyocyte Injury by Regulating the p38/p53 Pathway. Mediators Inflamm 2022;2022:1478181.
11. Yu M, Xie W, Tang Z, et al. Radiopaque and X-ray-Responsive Nanomedicine for Preventive Therapy of Radiation-Induced Heart Disease. Small 2023;19:e2303803.
12. Musa AE, Shabeeb D. Radiation-Induced Heart Diseases: Protective Effects of Natural Products. Medicina (Kaunas) 2019;55:126.
13. Rezaeyan A, Haddadi GH, Hosseinzadeh M, et al. Radioprotective effects of hesperidin on oxidative damages and histopathological changes induced by X-irradiation in rats heart tissue. J Med Phys 2016;41:182-91.
14. Najafi M, Shirazi A, Motevaseli E, et al. The melatonin immunomodulatory actions in radiotherapy. Biophys Rev 2017;9:139-48.
15. Farhood B, Aliasgharzadeh A, Amini P, et al. Radiation-Induced Dual Oxidase Upregulation in Rat Heart Tissues: Protective Effect of Melatonin. Medicina (Kaunas) 2019;55:317.
16. Fernandez-Gil BI, Guerra-Librero A, Shen YQ, et al. Melatonin Enhances Cisplatin and Radiation Cytotoxicity in Head and Neck Squamous Cell Carcinoma by Stimulating Mitochondrial ROS Generation, Apoptosis, and Autophagy. Oxid Med Cell Longev 2019;2019:7187128.
17. Pedre B, Barayeu U, Ezeriņa D, et al. The mechanism of action of N-acetylcysteine (NAC): The emerging role of H(2)S and sulfane sulfur species. Pharmacol Ther 2021;228:107916.
18. Schlaak RA, SenthilKumar G, Boerma M, et al. Advances in Preclinical Research Models of Radiation-Induced Cardiac Toxicity. Cancers (Basel) 2020;12:415.
19. Spitz DR, Azzam EI, Li JJ, et al. Metabolic oxidation/reduction reactions and cellular responses to ionizing radiation: a unifying concept in stress response biology. Cancer Metastasis Rev 2004;23:311-22.
20. Azzam EI, Jay-Gerin JP, Pain D. Ionizing radiation-induced metabolic oxidative stress and prolonged cell injury. Cancer Lett 2012;327:48-60.
21. Taunk NK, Haffty BG, Kostis JB, et al. Radiation-induced heart disease: pathologic abnormalities and putative mechanisms. Front Oncol 2015;5:39.
22. Kim W, Lee S, Seo D, et al. Cellular Stress Responses in Radiotherapy. Cells 2019;8:1105.
23. Schieber M, Chandel NS. ROS function in redox signaling and oxidative stress. Curr Biol 2014;24:R453-62.
24. Bresciani G, da Cruz IB, González-Gallego J. Manganese superoxide dismutase and oxidative stress modulation. Adv Clin Chem 2015;68:87-130.
25. Kudin AP, Bimpong-Buta NY, Vielhaber S, et al. Characterization of superoxide-producing sites in isolated brain mitochondria. J Biol Chem 2004;279:4127-35.
26. Lambert AJ, Brand MD. Inhibitors of the quinone-binding site allow rapid superoxide production from mitochondrial NADH:ubiquinone oxidoreductase (complex I). J Biol Chem 2004;279:39414-20.
27. Newmeyer DD, Ferguson-Miller S. Mitochondria: releasing power for life and unleashing the machineries of death. Cell 2003;112:481-90.
28. Spinelli JB, Haigis MC. The multifaceted contributions of mitochondria to cellular metabolism. Nat Cell Biol 2018;20:745-54.
29. Dröse S, Brandt U, Wittig I. Mitochondrial respiratory chain complexes as sources and targets of thiol-based redox-regulation. Biochim Biophys Acta 2014;1844:1344-54.
30. Halestrap AP. What is the mitochondrial permeability transition pore? J Mol Cell Cardiol 2009;46:821-31.
31. Briston T, Selwood DL, Szabadkai G, et al. Mitochondrial Permeability Transition: A Molecular Lesion with Multiple Drug Targets. Trends Pharmacol Sci 2019;40:50-70.
32. Whittington HJ, Ostrowski PJ, McAndrew DJ, et al. Over-expression of mitochondrial creatine kinase in the murine heart improves functional recovery and protects against injury following ischaemia-reperfusion. Cardiovasc Res 2018;114:858-69.
33. Giorgi C, Marchi S, Simoes ICM, et al. Mitochondria and Reactive Oxygen Species in Aging and Age-Related Diseases. Int Rev Cell Mol Biol 2018;340:209-344.
34. Assaly R, de Tassigny Ad, Paradis S, et al. Oxidative stress, mitochondrial permeability transition pore opening and cell death during hypoxia-reoxygenation in adult cardiomyocytes. Eur J Pharmacol 2012;675:6-14.
35. Piperno E, Berssenbruegge DA. Reversal of experimental paracetamol toxicosis with N-acetylcysteine. Lancet

1976;2:738-9.
36. Prescott LF, Park J, Ballantyne A, et al. Treatment of paracetamol (acetaminophen) poisoning with N-acetylcysteine. Lancet 1977;2:432-4.
37. Tenório MCDS, Graciliano NG, Moura FA, et al. N-Acetylcysteine (NAC): Impacts on Human Health. Antioxidants (Basel) 2021;10:967.
38. Smith TA, Kirkpatrick DR, Smith S, et al. Radioprotective agents to prevent cellular damage due to ionizing radiation. J Transl Med 2017;15:232.
39. Eligini S, Porro B, Aldini G, et al. N-Acetylcysteine Inhibits Platelet Function through the Regeneration of the Non-Oxidative Form of Albumin. Antioxidants (Basel) 2022;11:445.
40. Lu SC. Regulation of glutathione synthesis. Mol Aspects Med 2009;30:42-59.
41. Hinson JA, Monks TJ, Hong M, et al. 3-(glutathion-S-yl)acetaminophen: a biliary metabolite of acetaminophen. Drug Metab Dispos 1982;10:47-50.
42. van de Straat R, de Vries J, Debets AJ, et al. The mechanism of prevention of paracetamol-induced hepatotoxicity by 3,5-dialkyl substitution. The roles of glutathione depletion and oxidative stress. Biochem Pharmacol 1987;36:2065-70.
43. Chatterjee N, Walker GC. Mechanisms of DNA damage, repair, and mutagenesis. Environ Mol Mutagen 2017;58:235-63.
44. Sazonova EV, Petrichuk SV, Kopeina GS, et al. A link between mitotic defects and mitotic catastrophe: detection and cell fate. Biol Direct 2021;16:25.
45. Yamamoto Y, Minami M, Yoshida K, et al. Irradiation Accelerates Plaque Formation and Cellular Senescence in Flow-Altered Carotid Arteries of Apolipoprotein E Knock-Out Mice. J Am Heart Assoc 2021;10:e020712.
46. Kim KS, Kim JE, Choi KJ, et al. Characterization of DNA damage-induced cellular senescence by ionizing radiation in endothelial cells. Int J Radiat Biol 2014;90:71-80.
47. Philipp J, Le Gleut R, Toerne CV, et al. Radiation Response of Human Cardiac Endothelial Cells Reveals a Central Role of the cGAS-STING Pathway in the Development of Inflammation. Proteomes 2020;8:30.
48. Yilmaz H, Mercantepe F, Tumkaya L, et al. The potential antioxidant effect of N-acetylcysteine on X-ray ionizing radiation-induced pancreas islet cell toxicity. Biochem Biophys Res Commun 2023;685:149154.
49. Kim HJ, Kang SU, Lee YS, et al. Protective Effects of N-Acetylcysteine against Radiation-Induced Oral Mucositis In Vitro and In Vivo. Cancer Res Treat 2020;52:1019-30.
50. Mercantepe T, Topcu A, Rakici S, et al. The radioprotective effect of N-acetylcysteine against x-radiation-induced renal injury in rats. Environ Sci Pollut Res Int 2019;26:29085-94.

Cite this article as: Li YL, Wang G, Wang BW, Li YH, Ma YX, Huang Y, Yan WT, Xie P. The potential treatment of N-acetylcysteine as an antioxidant in the radiation-induced heart disease. Cardiovasc Diagn Ther 2024;14(4):509-524. doi: 10.21037/cdt-24-19